Morphology of Micropitting

R. L. Errichello

Understanding the morphology of micropitting is critical in determining the root cause of failure. Examples of micropitting in gears and rolling-element bearings are presented to illustrate morphological variations that can occur in practice.

General Morphology

To the unaided eye, micropitting appears dull, etched or stained, with patches of gray. Micropitting is difficult to see under diffuse fluorescent lighting and is best observed with intense directional lighting. A flashlight with a concentrated beam held in the proper direction effectively illuminates micropitting. With intense lighting, micropitting might sparkle or appear speckled. Figure 1 is a scanning electron microscopy (SEM) image that shows the floor of a micropit crater sloping gently downward from its origin at the tooth surface. The floor has a rough surface typical of that caused by ductile-fatigue-crack propagation. A feather-edge forms at the back of the crater due to plastic flow of material over the crater rim. The feather-edge appears white in SEM when it becomes charged with electrons. Material surrounding a micropit generally appears smooth and featureless, unless abraded.

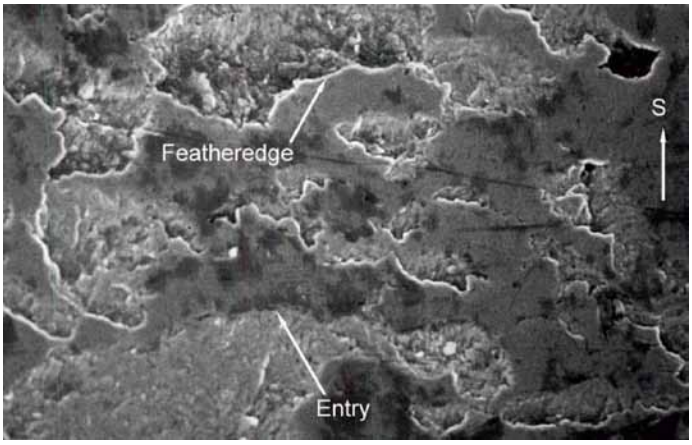

Figure 1 SEM image of micropitting.

Gear Tooth Sliding

Figure 2 shows the directions of the rolling (R) and sliding (S) velocities on the driving and driven gear teeth. Contact on the driver tooth starts near the root of the tooth, rolls up the tooth, and ends at the tooth tip. Sliding is away from the driving gear pitch line. Contact on the driven tooth starts at the tooth tip, rolls down the tooth, and ends near the tooth root. Sliding is towards the driven gear pitch line. Like macropitting, micropitting cracks grow opposite the direction of sliding at the gear tooth surface. Consequently, the cracks converge near the pitch line of the driver and diverge near the pitch line of the driven gear.

Figure 3 shows metallurgical sections cut transversely through micropits that show cracks start at or near the gear tooth surface and grow at a shallow angle (typically 10–30°, but sometimes as steep as 45°) to the surface.

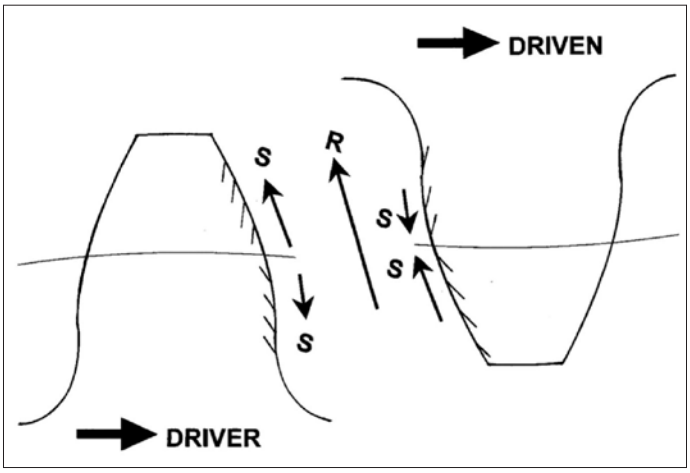

Figure 2 Rolling (R) and sliding (S) directions.

Hydraulic Pressure Propagation

Gear teeth dedenda have negative sliding; i.e., direction of rolling velocity is opposite sliding velocity. Negative sliding is significant because it promotes Hertzian fatigue by allowing oil to enter surface cracks where it accelerates crack growth by the hydraulic-pressure-propagation mechanism first proposed by Stewart Way (Ref. 1) and verified many times by experiments such as Littmann's (Ref. 2).

Figure 4 shows profile inspection charts that demonstrate typical profile damage due to micropitting on the drive flanks of a wind turbine high-speed (HS) pinion.

The charts for the coast flanks show the original accuracy of the pinion was high, but the micropitting caused severe deterio-

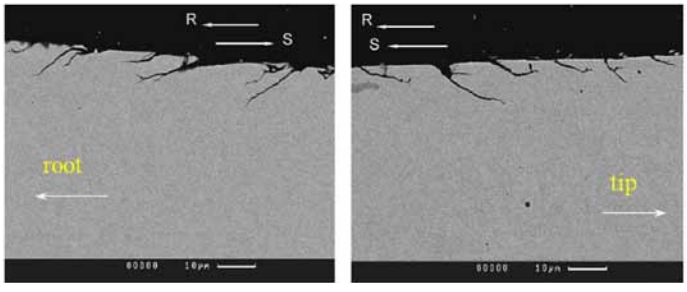

Figure 3 Micropitting cracks on a driven gear (courtesy of Newcastle University).

ration of the drive flanks. Note that the entire active drive flanks were damaged, but the damage was most severe in the dedenda in the area of negative sliding.

Figure 5 shows a form-ground wind turbine intermediate (INT) pinion with micropitting that crosses the pitch line.

Because slide directions reverse as the pitch line is crossed, micropitting cracks grow in opposite directions above and below the pitch line. Figure 5 shows that when micropitting grows across the pitch line, it makes the pitch line readily discernible because opposite inclinations of the floors of micropit craters scatter light in opposite directions above and below the pitch line.

Surface Topography

Figure 6 is an SEM image of micropitting on a high asperity of a ground tooth surface.

Micropitting begins by attacking high points on gear tooth surfaces such as crests of undulations, peaks of cutter scallops, ridges of grinding lay, and edges of grinding scratches. Figure 6 shows the surface of the asperity has been severely plastically deformed. Tractional stress from sliding has caused material to flow over the micropit craters and form a featheredge at the exit side of the craters. Growth of the micropits is opposite to the slide direction and begins at the entry (first point reached by the roll direction) and ends at the exit (last point reached by the roll direction).

Figure 7 shows a skive-hobbed wind turbine low speed (LS) wheel with micropitting on peaks of the hob scallops. Figure 8 shows a form-ground wind turbine INT wheel with micropitting on peaks of longitudinal grind scratches. Multiple cracks originate at these sites and coalesce to form micropits along lines that follow high points of surface topography. If ridges are periodic, micropitting might form in regularly spaced rows. Micropitting generally progresses until surface peaks are removed, and might continue until large areas of tooth surface become porous and continuously cracked.

Figure 8 shows a form-ground wind turbine INT wheel with micropitting on peaks of longitudinal grind scratches.

Gear teeth dedenda are vulnerable to micropitting, especially along the start of active profile (SAP) and the lowest point of single tooth pair contact (LPSTC). However, micropitting might occur anywhere on active flanks. Micropitting might occur at edges of teeth, at boundaries of surface defects such as scratches and debris dents, adjacent to damage from other failure modes such as macropitting or scuffing, and wherever the elasto-hydrodynamic lubrication (EHL) film is disrupted.

Micropitting Patterns

If the pinion and wheel were initially accurate and had little run-out, micropitting damage might be similar from tooth-to-tooth. In these cases micropitting patterns can be interpreted in much the same way contact patterns are used to assess gear tooth alignment and load distribution. For example, Figure 9 shows a helical wheel that had some misalignment.

When micropitting damage varies from tooth-to-tooth, it usually means there are tooth-to-tooth variations in tooth geometry or surface roughness. Gear sets with non-hunting gear ratios might develop micropitting patterns that repeat at

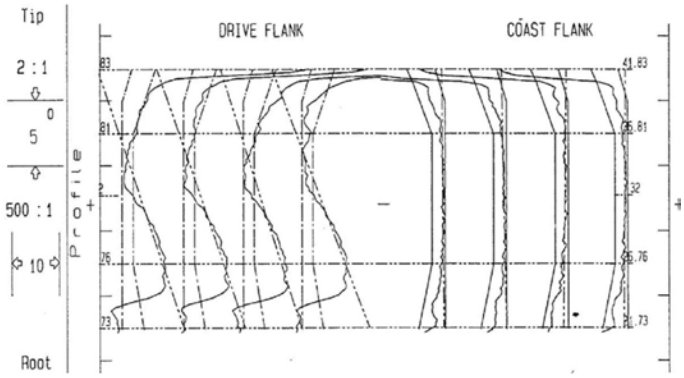

Figure 4 Typical profile damage due to micropitting on wind turbine HS pinion.

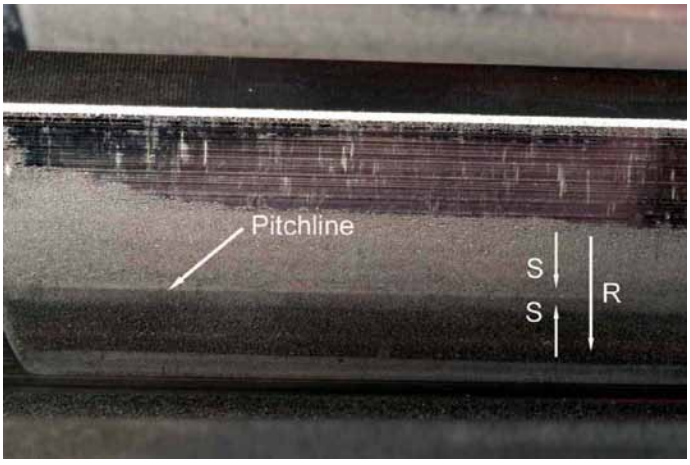

Figure 5 Pitch line is readily discernible on a driven wind turbine INT pinion.

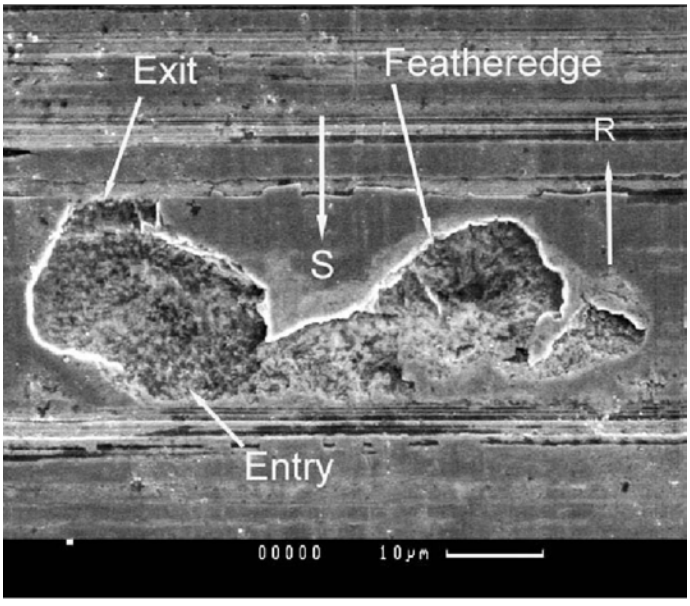

Figure 6 SEM image of micropitting on asperity peak of ground tooth surface (courtesy of Newcastle University).

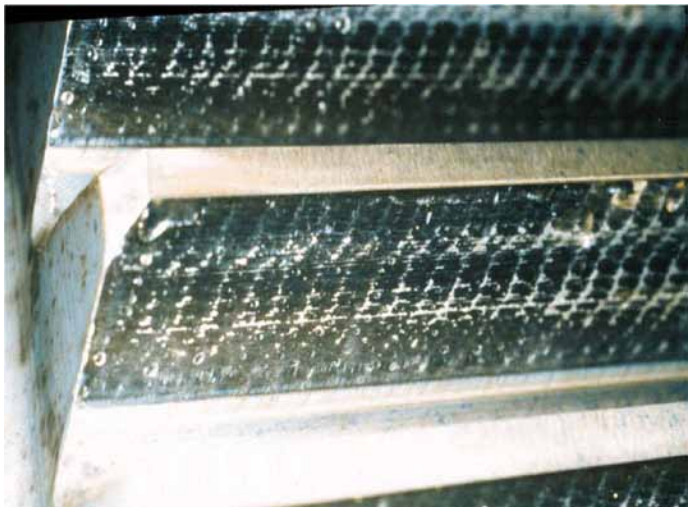

Figure 7 Wind turbine LS wheel with micropitting on peaks of hob scallops.

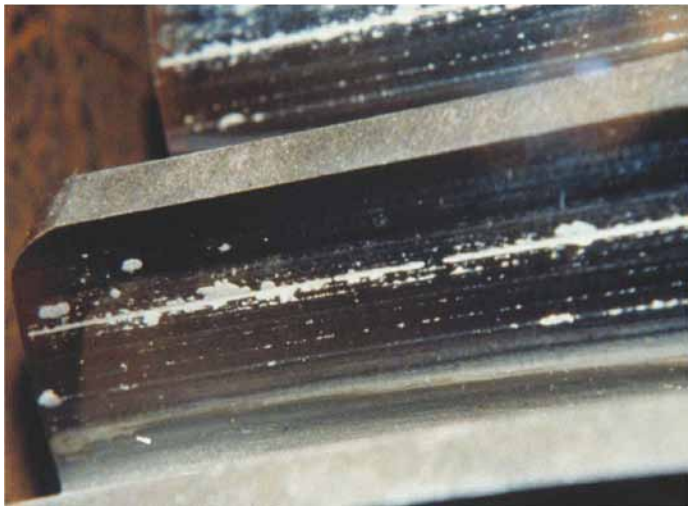

Figure 8 Wind turbine INT wheel with micropitting on peaks of grind scratches.

Figure 9 Micropitting pattern on a helical wheel that had some misalignment (courtesy of Caterpillar).

the frequency of a common factor of the tooth combination. For example, a gear set with a 25/55-tooth combination, and a common factor of five, might have similar micropitting on every fifth tooth.

There might be micropitting only on the pinion, only on the wheel, or on both. Generally, the gear with the roughest surface causes micropitting on the mating gear, especially if it is harder than the mating gear. Micropitting is most damaging when the opposing surface is rough, harder and faster. Micropitting resistance improves when the harder surface is made smooth. A worst case example would be a sun pinion that mates with multiple planet wheels that are rougher and harder than the sun pinion.

Geometric Stress Concentration (GSC)

Micropitting might occur at GSC such as:

- Edges of gear teeth
- Ends of bearing rollers
- Boundaries of surface defects such as macropitting, scuffing, fretting corrosion, or debris dents
- Tip-to-root interference at the SAP
- Corners of tip relief
- Wherever the EHL film is disrupted

Figure 10 shows a form-ground wind turbine HS pinion with micropitting at the edge of contact at the drive end of the active face width.

Figure 11 shows a form-ground wind turbine sun pinion with micropitting on shoulders of debris dents. Debris dents are local depressions that cause loss of EHL film thickness and lead to GSC at shoulders of dents. Cyclic contacts at these sites generate pressure spikes, plastic deformation, and tensile residual stresses that eventually initiate micropits.

Debris dents on rolling-element bearing raceways usually cause micropitting that frequently initiates point-surface-origin (PSO) macropitting. Therefore, debris dents are a common root cause of bearing failure.

Figure 12 shows a shaved automotive planet wheel. In addition, Figure 12 shows micropitting at edges of a PSO macropit. It is a secondary failure mode that occurred because the PSO macropit disrupted the EHL lubricant film. Other teeth show there is also micropitting on peaks of the shaving marks.

Figure 13 shows a FZG PT-C pinion with a PSO macropit that initiated at the cusp above tip-to-root damage at the SAP.

The root cause of the PSO macropit shown in Figure 13 is GSC caused by tip-to-root interference (Ref. 3). The FVA micropitting test (Ref. 4) requires the test to be terminated when a macropit occurs.

Figure 14 shows a FZG GF–C pinion with a PSO macropit that initiated at the upper edge of a 2 mm-high band of micropitting.

The root cause of the PSO macropit shown in Figure 14 is GSC caused by micropitting (Ref. 5).

FZG GF-C gears (Ref. 4) are the same as FZG PT–C gears in all respects except PT–C gears have a tooth surface roughness of Ra = 0.3 µm, whereas GF–C gears have tooth surface roughness of Ra = 0.5 µm. The rougher surfaces of GF–C gears cause more severe micropitting that removes the cusp at the SAP due to tip-to-root interference and prevents initiation of PSO mac-

ropitting at the SAP. Therefore, the micropitting prolongs the macropitting life until the micropitting spreads to the pitchline, where PSO macropits initiate at the top of the micropitting band because of GSC caused by the step in the tooth profile at the upper edge of the micropitting crater (Ref. 6). Consequently, in the FZG GF–C test, a lubricant with superior micropitting resistance might give a shorter macropitting life than a lubricant with inferior micropitting resistance.

Figure 15 shows a contact line with fretting corrosion on a wind turbine INT wheel, as well as micropitting at edges of the fretting line. The fretting corrosion occurred when the wind turbine was parked; the micropitting occurred later during operation due to GSC at the edges of the fretting line. Therefore, fretting corrosion was the primary failure mode and micropitting was a secondary failure mode.

Micropitting in Rolling-Element Bearings

Figure 16 shows micropitting on the inner ring (IR) of a cylindrical roller bearing (CRB) from a wind turbine HS pinion. The micropitting reduced the diameter of the IR, increased the bearing internal clearance, increased the roller loads, and increased stresses. Furthermore, the micropitting caused the IR to conform to the rollers and negate the crown of the rollers. This caused GSC at the ends of the rollers and resulted in macropitting at each end of the raceway. Therefore, micropitting was the primary failure mode and GSC macropitting was a secondary failure mode.

Figure 17 is an SEM image of the central part of Figure 16, showing an enlarged view of the micropitting.

Figure 17 shows that micropitting in rolling-element bearing components has a directional randomness that differs from the more directionally oriented micropitting that is typical in gear teeth. This is probably caused by differences in sliding directions, which are more random in rolling-element bearings than in gears.

Figure 18 shows a roller from a CRB from a wind turbine INT pinion. The roller has scuffing in two circumferential bands that were caused by skidding between the roller and the outer ring (OR) raceways.

The bearing has a disc-shaped cage that is guided by a groove in the two-piece OR. No contact occurs between the roller and OR raceway in the central portion of the roller because the OR raceway is interrupted by the cage groove. Consequently, no scuffing occurred in the central portion of the roller. Furthermore, the roller has end-reliefs that prevented scuffing at the roller ends.

Figure 19 shows a CRB IR from a wind turbine INT pinion that mated with the roller shown in Figure 18.

Figure 19 shows micropitting that occurred in two circumferential bands—separated by a central band without micropitting. The two bands of micropitting were caused by the scuffing-induced roughness on the rollers. There is also a band without micropitting at each end of the active raceway; GSC macropitting occurred on the left and central bands.

Figure 20 is a plot of the axial profile of the IR shown in Figure 19.

Figure 20 shows the micropitting caused two ruts in the raceway that are up to 64 µm deep. Consequently, a major portion

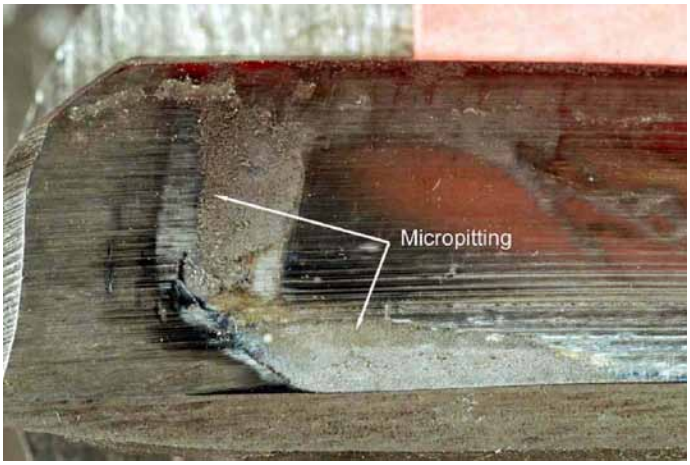

Figure 10 Wind turbine HS pinion with micropitting at edge of contact.

Figure 11 Wind turbine sun pinion with micropitting on shoulders of debris dents.

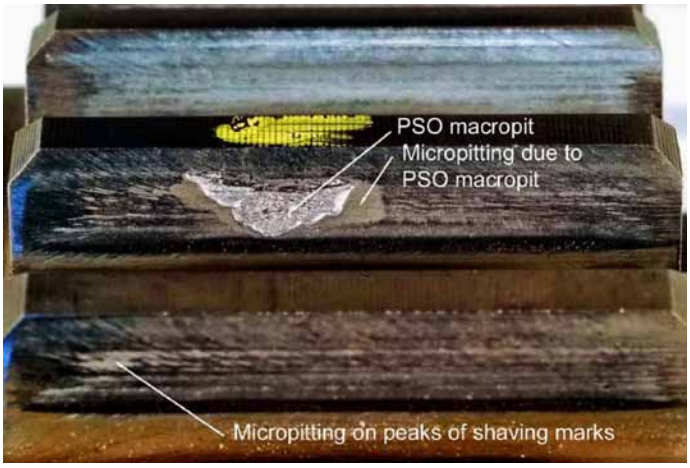

Figure 12 Micropitting at edges of PSO macropit on shaved automotive planet.

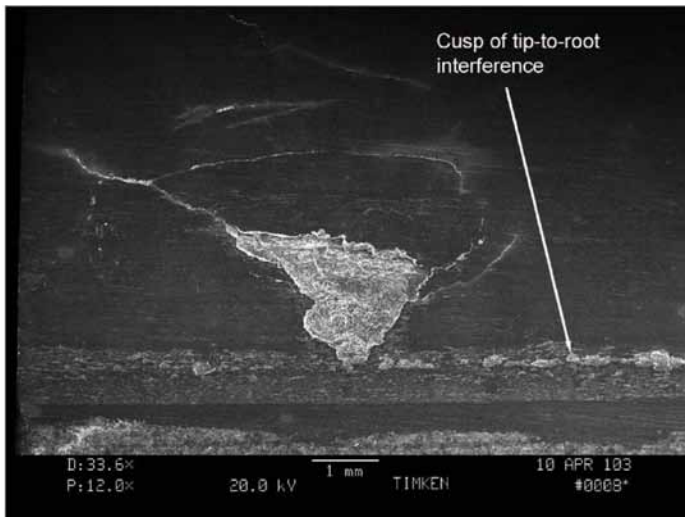

Figure 13 FZG PT–C pinion with PSO macropit starting from GSC at SAP (courtesy of Afton Chemical).

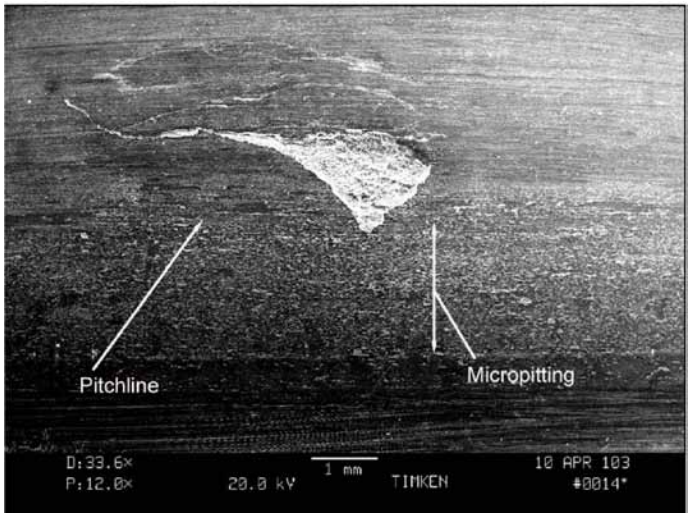

Figure 14 FZG GF–C pinion with PSO macropit starting from GSC near pitch line (courtesy of Afton Chemical).

Figure 15 Wind turbine INT wheel with micropitting at edges of fretting line.

of the load-bearing area of the IR raceway was lost, leaving only the central part of the raceway and two ends to support load; this in turn led to the GSC macropitting (Fig. 19).

This example demonstrates a complex series of failure modes that started with scuffing between the rollers and OR raceway; this was followed by micropitting on the IR raceway caused by the rough surfaces of the scuffed rollers, and, finally, GSC macropitting on the IR caused by GSC due to micropitting. Therefore, scuffing was the primary failure mode and micropitting and GSC macropitting were secondary failure modes.

Figure 21 shows the influence of oil type on micropitting. The test results were obtained with AGMA test gears (Ref. 7). The pinion and wheel have tip relief, and the pinion has a crown that limits the size of the contact pattern.

Influence of Lubricant Properties

Figure 21 shows Oil-A had the lowest micropitting resistance and Oil-E had the highest micropitting resistance. Oil-A and Oil-B initiated macropitting due to GSC at the top of the micropitting band. Oil-F had the second-best micropitting resistance, but a PSO macropit initiated due to GSC caused by tip-to-root interference.

Micropitting resistance is strongly affected by lubricant properties—especially the base oil type, viscosity at the operating temperature, viscosity-pressure coefficient (Ref. 8) and the lubricant chemistry. Anti-wear additives are generally detrimental to micropitting resistance, primarily because they inhibit run-in and preserve damaging roughness. However, some friction-reducing additives are beneficial (Ref. 9).

Oil cleanliness must be maintained to avoid micropitting caused by debris dents (Ref. 10). Furthermore, gearbox inspections have shown that water contamination promotes micropitting in gears and bearings, and experiments (Ref. 11) have shown that water contamination can significantly reduce the anti-corrosion, film formation, and friction-reducing properties of oil.

Influence of Metallurgy

Gears have maximum micropitting resistance when made from steel with sufficient hardenability to obtain microstructures consisting primarily of tempered martensite. Retained austenite of about 20% is thought to be beneficial. Retained austenite greater than 30% generally reduces hardness, strength and compressive residual stress in carburized gears, and is therefore detrimental to micropitting resistance.

Carburized gears are usually hobbed, carburized, hardened and ground, so their tribological properties depend on characteristics of ground surfaces. But some carburized, nitrided and induction-hardened gears are not ground after hardening, and their surfaces may be hard and rough. These surfaces are likely to produce micropitting on mating gears. However, if heat treat distortion is adequately controlled—and tooth surfaces are smooth—heat-treated surfaces can be resistant to micropitting. Oxidation at the surface and along grain boundaries might actually be beneficial. The oxide layer formed during heat treatment might provide boundary-film protection similar to a solid lubricant and provide protection during run-in.

Conclusions

- Understanding the morphology of micropitting is the key to determining the primary failure mode and root cause of failure.
- Like macropitting, micropitting cracks grow opposite the direction of sliding at the gear tooth surface. Consequently, the cracks converge near the pitch line of the driver and diverge near the pitch line of the driven gear.
- Metallurgical sections cut transversely through micropits show that cracks start at or near the gear tooth surface and grow at a shallow angle—typically 10–30°, but sometimes as steep as 45° to the surface.
- Gear teeth dedenda have negative sliding; i.e., the direction of rolling velocity is opposite sliding velocity. Negative sliding is significant because it promotes Hertzian fatigue by allowing oil to enter surface cracks where it accelerates crack growth by the hydraulic-pressure-propagation mechanism.
- Because slide directions reverse as the pitch line is crossed, micropitting cracks grow in opposite directions above and below the pitch line. When micropitting grows across the pitch line it makes the pitch line readily discernible because opposite inclinations of the floors of micropit craters scatter light in opposite directions above and below the pitch line.
- Micropitting begins by attacking high points on gear tooth surfaces such as crests of undulations, peaks of cutter scallops, ridges of grinding lay, and edges of grinding scratches. Tractional stress from sliding causes material to flow over the micropit craters and form a feather-edge at the exit-side of the craters.
- If the pinion and wheel were initially accurate and had little run-out, micropitting damage might be similar from tooth to tooth. In these cases micropitting patterns can be interpreted in much the same way contact patterns are used to assess gear tooth alignment and load distribution.
- When micropitting damage varies from tooth to tooth, it usually means there are tooth-to-tooth variations in tooth geometry or surface roughness. Gear sets with non-hunting gear ratios might develop micropitting patterns that repeat at the frequency of a common factor of the tooth combination. For example, a gear set with a 25/55–tooth combination, and a common factor of five, might have similar micropitting on every fifth tooth.
- There might be micropitting only on the pinion, only on the wheel—or both. Generally, the gear with the roughest surface causes micropitting on the mating gear—especially if it is harder than the mating gear.

Micropitting is most damaging when the opposing surface is rough, harder and faster; micropitting resistance improves when the harder surface is made smooth.

Micropitting might occur at GSC such as:

- Edges of gear teeth
- Ends of bearing rollers
- Boundaries of surface defects, such as macropitting, scuffing, fretting corrosion, or debris dents
- Tip-to-root interference at the SAP
- Corners of tip relief
- Wherever the EHL film is disrupted
- Micropitting in rolling-element bearing components has a directional randomness that is different from the more directionally oriented micropitting typical in gear teeth. This is probably caused by differences in sliding directions, which are more random in rolling-element bearings than in gears.

Figure 16 Micropitting on CRB IR of wind turbine HS pinion.

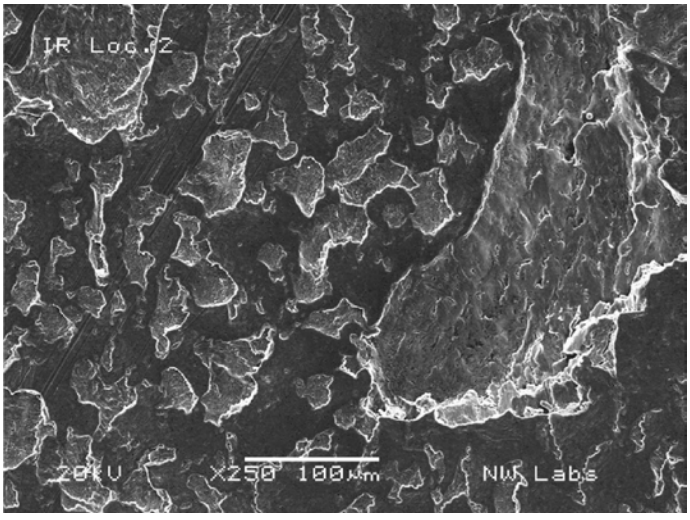

Figure 17 SEM image of micropitting on pinion (courtesy of Northwest Labs).

Figure 18 Scuffing on CRB roller from wind turbine INT pinion bearing.

- Micropitting resistance is strongly affected by lubricant properties, especially the base oil type, viscosity at the operating temperature, and the lubricant chemistry. Anti-wear additives are generally detrimental to micropitting resistance primarily because they inhibit run-in and preserve damaging roughness. However, some friction-reducing additives are beneficial.
- Oil cleanliness must be maintained to avoid micropitting caused by debris dents. Furthermore, water contamination promotes micropitting in gears and bearings, and significantly reduces the anticorrosion, film formation and friction-reducing properties of oil.
- With FZG PT–C gears, PSO macropits initiate at the cusp formed by tip-to-root interference, whereas With FZG GF–C gears, their rougher surfaces cause more severe micropitting that removes the cusp at the SAP and thereby prolongs the macropitting life until PSO macropitting occurs near the pitchline because of GSC caused by the step in the tooth profile at the upper edge of the micropitting crater. Consequently, in the FZG GF–C test, a lubricant with superior micropitting resistance might give a shorter macropitting life than a lubricant with inferior micropitting resistance.

Table 1—Metallurgy and finished method

Figure No.	Steel alloy	Heat treatment	Surface hardness	Finishing method
5	17CrNiMo6	Carburize	59 HRC	Form ground
6	17CrNiMo6	Carburize	58 HRC	Form ground
7	AISI 4320H	Carburize	59 HRC	Skive hobbed
8	17CrNiMo6	Carburize	58 HRC	Form ground
9	AISI 8620H	Carburize	58 HRC	Shaved
10	AISI 9310H	Carburize	60 HRC	Form ground
11	17CrNiMo6	Carburize	59 HRC	Form ground
12	AISI 8620H	Carburize	58 HRC	Shaved
13	16MnCr5	Carburize	60 HRC	MAAG 0° ground
14	16MnCr5	Carburize	60 HRC	MAAG 0° ground
15	17CrNiMo6	Carburize	60 HRC	Form ground
16	AISI 52100	Though hard	60 HRC	Ground
17	AISI 52100	Though hard	60 HRC	Ground
18	AISI 52100	Though hard	60 HRC	Ground
19	AISI 52100	Though hard	60 HRC	Ground
21	AISI 8620H	Carburize	58 HRC	Form ground

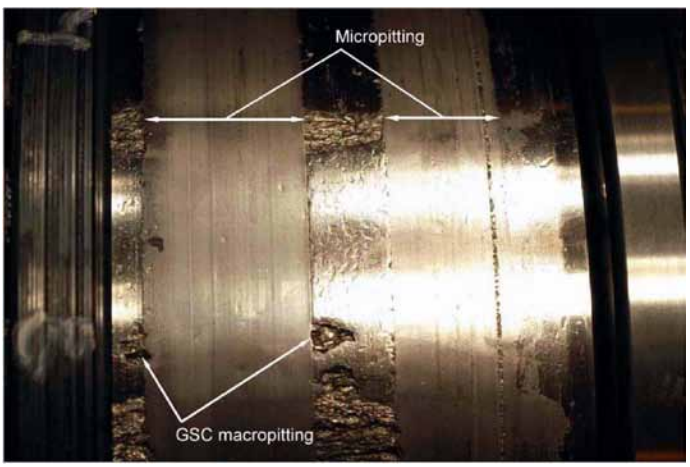

Figure 19 Micropitting on CRB IR from a wind turbine INT pinion bearing.

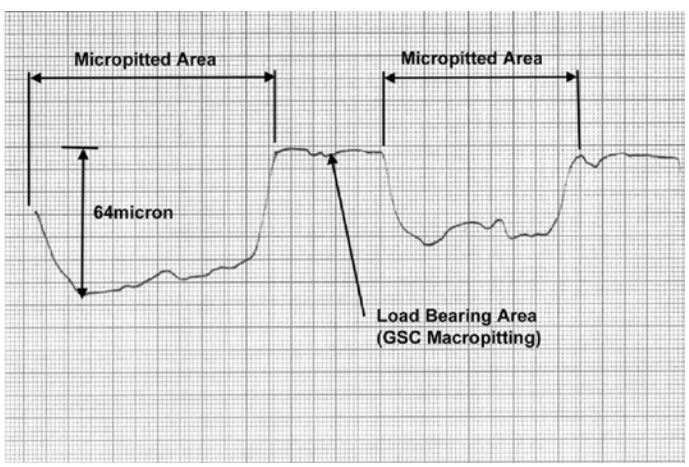

Figure 20 Axial profile of CRB IR from wind turbine INT bearing.

- Gears have maximum micropitting resistance when made from steel with sufficient hardenability to obtain microstructures consisting primarily of tempered martensite. Retained austenite of about 20% is thought to be beneficial.

References

1. Way, S. "Pitting Due to Rolling Contact," ASME Trans., *Journal of Applied Mechanics, Vol. 57*, pp. A49–A114, 1935.
2. Littmann, W. E. "The Mechanism of Contact Fatigue—An Interdisciplinary Approach to the Lubrication of Concentrated Contacts," SP–237, NASA, pp. 309–377, 1970.
3. Errichello, R.L., C. Hewette and R. Eckert. "Point-Surface-Origin Macropitting Caused by Geometric Stress Concentration," AGMA Paper 10FTM11, Oct., 2010.
4. FVA Information Sheet. "Micropitting," No. 54/7, July 1993, Forschungsvereinigung Antriebstechnik e.V., Lyoner Strasse 18, D–60528 Frankfurt/Main, pp. 1–8, 1993.
5. Jao, T.C., et al. "Influence of Surface Roughness on Gear Pitting Behavior," AGMA Paper 04FTM4, Oct. 2004.
6. Li, S., et al. "Investigation of Pitting Mechanism in the FZG Pitting Test," SAE Paper 2003–01–3233, 2003.
7. Buzdygon, K.J. and A.B. Cardis. "A Short Procedure to Evaluate Micropitting Using the New AGMA-Designed Gears," AGMA Paper 04FTM7, Oct., 2004.
8. Errichello, R. "Selecting Oils with High-Pressure-Viscosity Coefficient," *Machinery Lubrication, Vol. 4, No. 2*, pp. 48–52, Mar.–Apr. 2004.
9. Laine, E., A.V. Olver, M.F. Lekstrom, B.A. Shollock, T.A. Beveridge and D.Y. Hua. "The Effect of a Friction Modifier Additive on Micropitting," *Tribology Transactions, Vol. 52, No. 4,* pp. 526–533, Jul.–Aug. 2009.
10. Errichello, R. and J. Muller. "Oil Cleanliness in Wind Turbine Gearboxes," *Machinery Lubrication, Vol. 2, No. 4,* pp. 34–40, Jul.–Aug. 2002.
11. Devlin, M., et al. "The Effect of Water Contamination and Oxidation on the Fatigue Life Performance of Wind Turbine Lubricants," presented at the NLGI 70th Annual Meeting, Hilton Head Island, SC, pp. 1–10, Oct. 26–29, 2003.

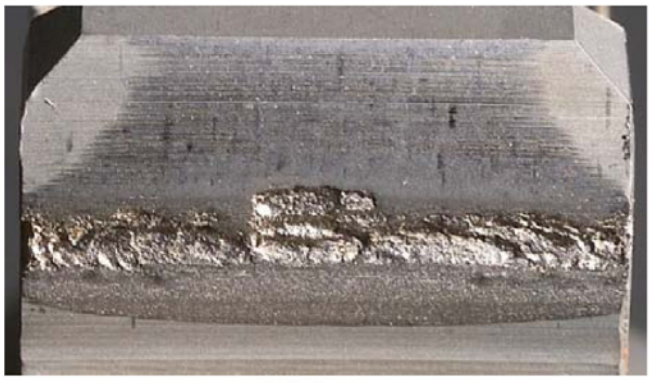

Oil A

Oil B

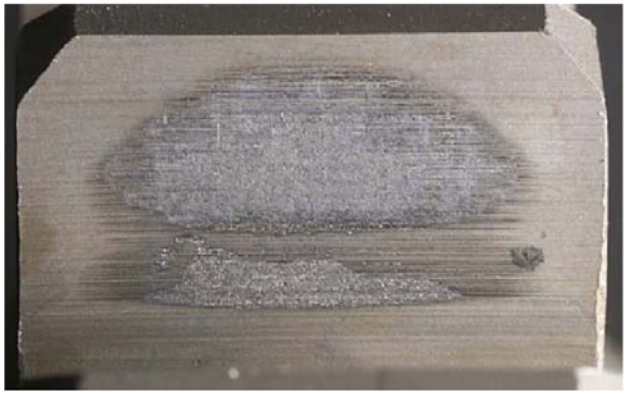

Oil C

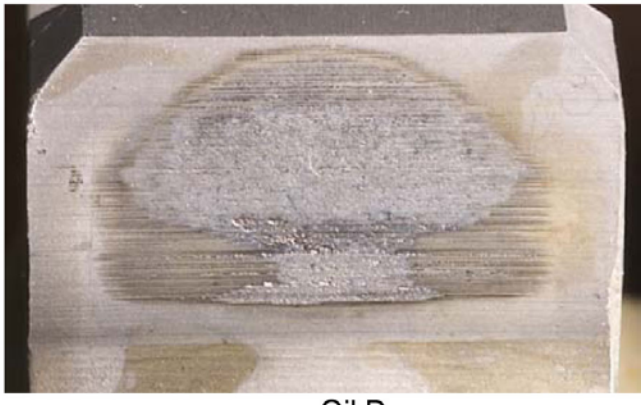

Oil D

Oil E

Oil F

Oil G

Figure 21 Influence of oil type on micropitting (courtesy of ExxonMobil).

Robert Errichello, PE, heads his own gear consulting firm—GEARTECH—and is a founder of GEARTECH Software, Inc. A graduate of the University of California at Berkeley, he holds B.S. and M.S. degrees in mechanical engineering and a master of engineering degree in structural dynamics. In his more than 30 years of industrial experience, Errichello worked for several gear companies; he has also been a consultant to the gear industry for more than 20 years and has taught courses in material science, fracture mechanics, vibration and machine design at San Francisco State University and the University of California at Berkeley. He is also a member of ASM International, STLE, ASME Power Transmission and Gearing Committee, AGMA Gear Rating Committee and the AGMA/AWEA Wind Turbine Committee. Errichello has published dozens of articles on design, analysis and the application of gears, and is the author of three widely used computer programs for the design and analysis of gears. He is also a longtime technical editor for *Gear Technology* magazine and STLE Tribology Transactions, and has presented numerous seminars on design, analysis, lubrication and failure analysis of gears. Errichello is a past recipient of the AGMA TDEC award and the STLE Wilbur Deutch Memorial award.